Journal of Applied Electrochemistry **32**: 743–753, 2002.
© 2002 *Kluwer Academic Publishers. Printed in the Netherlands.*

Copper electrodeposition from a pH 3 sulfate electrolyte

A. VICENZO and P.L. CAVALLOTTI*
Dipartimento di Chimica, Materiali e Ingegneria Chimica "Giulio Natta", Politecnico di Milano, via Mancinelli 7, 20131 Milan, Italy
*(*author for correspondence, fax: +39 02 23993180, e-mail: pietro.cavallotti@polimi.it)*

Received 17 December 2001; accepted in revised form 10 April 2002

Key words: copper electrodeposition, electrokinetics, interconnects, plating additives

Abstract

Kinetics and growth modes of copper electrodeposited from copper sulfate 0.8 M, pH 3 electrolytes are studied and compared to those for standard acidic sulfate baths. The influence of chlorides and three different additives (polyethylene glycol, a thiocompound and a quaternary ammonium salt) on steady state and transient electrokinetic behaviour, structure and morphology is investigated. Chlorides behave as a surface stabilizing agent, promoting epitaxy and contributing to the electrolyte microlevelling power. Each organic additive shows a specific effect which, however, may change substantially in the presence of other additives. Polyethylene glycol is a suppresser with the strongest action on copper electrodeposition, as shown by its effects on discharge kinetics and growth behaviour. The main role of the brightener (thiocompound) and the leveller (quaternary ammonium salt) consists in mitigating or tuning the surfactant blocking action respectively, realising the best balance between catalytic and suppressing factors. The pH 3 electrolyte is shown to be a valuable alternative to the standard acid bath, allowing higher deposition rates and promising improvements with regard to microthrowing power and growth control of thin films.

1. Introduction

Essential requirements for copper plating of ultrascale integrated interconnects are voids-free filling of trenches and vias and thickness distribution uniformity at wafer scale. The achievement of both results depends on different and related factors: in particular, overpotential distribution and concentration gradients at the surface. Phenomena controlling uniformity at micro and macro scale should be mastered through a careful selection of plating bath composition, including additives, and deposition rate. In this respect, a suitable choice of the base electrolyte composition (i.e., $CuSO_4$ and H_2SO_4 concentration) should be considered the starting point for improving plating performance.

The acid sulfate bath has become the standard electrolyte for copper plating in microelectronics for its long-lasting use in printed circuits manufacture. A 'low-acid' sulfate bath with high copper concentration was proposed by Landau [1], stressing its potential benefit with respect to standard electrolytes, thanks to conductivity decrease and copper transport rate enhancement. As discussed by Landau, lowering the electrolyte conductivity minimises the terminal effect due to the resistive seed layer, thus improving deposit uniformity. With regard to the ability to fill trenches and vias, the relative value of activation and concentration resistance is important [2], since both high metal cations concentration and low activation resistance at the bottom of the vias are desirable. Thus, high copper concentration is expected to be beneficial to via filling, as also stated in other recent reports [3, 4] and easily explained when the factors affecting deposit microdistribution are taken into consideration [5]. Actually, it was ascertained that increasing pH and copper sulfate concentration microroughness decreases [6], as a consequence of increasing copper transport number, that is, lowering concentration polarization has a beneficial effect on deposit microdistribution.

The standard copper plating bath for wafer metallization contains, besides H_2SO_4 to provide a high throwing power, a multicomponent additive system, especially formulated to achieve super-filling [7]. Additives selection must be optimized, since only their synergetic action produces the desired balance of inhibition and acceleration [8], particularly with regard to the topographic features of the patterned substrate. In the present study, the specific role of a set of additives, representative of the kind of addition agents employed in copper plating for interconnects, is investigated. Kinetic behaviour during deposition, structure and morphology of copper layers on blanket wafers are characterised and discussed with regard to additive influence.

2. Experimental details

Copper deposition was carried out from both $CuSO_4$ 0.25 M, H_2SO_4 1.5 M standard electrolyte and $CuSO_4$ 0.8 M electrolyte at pH 3. Plating baths were prepared with chemicals of analytical grade and distilled water; pH was adjusted with dilute H_2SO_4, when needed. Chloride traces in the starting solution were precipitated as AgCl by small addition of Ag_2CO_3 ($\sim$1 mM l^{-1}). After standing overnight, the solution was filtered, treated with active charcoal and electrolysed at low current density (cd) (<0.5 mA cm^{-2}) for about 24 h.

Silicon coated with a TiN/Cu stack was used as substrate throughout this work, apart from a few cases of deposition on polished brass. The sputtered copper layer was 100 nm thick with [111] texture; the brass substrate had a weak (100) texture. The anode was a large electrolytic copper plate. Electrodeposition was carried out in 300 ml prismatic Pyrex cells, without stirring, unless otherwise mentioned, at 20 mA cm^{-2}, 30 °C or 25 °C; layer thickness was 10 μm. Before plating, solutions were deaerated by nitrogen bubbling for about 30 min.

Four additives, namely Cl^- 50 ppm, dibenzyl-dithiocarbamate (TC) 8 ppm, 1500 MW polyethylene glycol (PEG) 300 ppm and a quaternary ammonium salt (trioctyl-methyl-ammonium chloride, QAS) 18 ppm, were studied (see Table 1 for plating bath compositions). After additives addition, a further low cd treatment (1 mA cm^{-2}) was carried out on solutions N and Q, while the other solutions were worked at the standard cd of 20 mA cm^{-2} until a sound copper layer was obtained.

Deposits structure was characterized by taking X-ray diffraction (XRD) patterns, with CuK_α radiation and a powder goniometer. To assess the degree of preferred orientation (PO), an estimate of the volume fraction of different texture components was obtained by the following equation [9, 10]:

$$M_{hkl} = F_{hkl} \times \left(\sum_{hkl} F_{hkl} \right)^{-1}$$

The values F_{hkl} are calculated according to the expression

$$F_{hkl} = n \times \frac{I_{hkl}}{I^R_{hkl}} \times \left(\sum_{hkl} \frac{I_{hkl}}{I^R_{hkl}} \right)^{-1}$$

where I_{hkl} is the measured intensity of reflection (hkl) and I^R_{hkl} is the reflection intensity of a random powder sample; n is the number of measured reflections. The calculation is based on the assumption that only crystals with orientation along (111), (100), (110), (311) directions occur.

Surface morphology of 10 μm thick coatings was studied by scanning electron microscopy (SEM). Contact atomic force microscopy (AFM) was used to characterize the early stages of growth onto Si/TiN/Cu substrate by imaging thin copper films topography after 30 s deposition at 20 mA cm^{-2} and 30 °C from bath B, E, G, H and N.

The influence of the different additives upon deposition kinetics was studied by steady state and transient electrochemical techniques.

Low scan linear sweep voltammograms were performed after deposition of a thin copper layer (20 mA cm^{-2}, 10 min) on Si/TiN/Cu (100 nm) substrate, with cathodic area about 0.15 cm^2, from deaerated solutions at 25 °C and under magnetic stirring. The potential was driven in the cathodic direction at scan rate of 0.2 mV s^{-1} from the open circuit potential (OCP) up to about 50 mA cm^{-2} end current. The Ag/AgCl (KCl 3 M) reference electrode (RE) was placed at about 5 mm from the working electrode and the recorded polarization curves were not corrected for uncompensated ohmic resistance. The pH 3 electrolyte conductivity is about 0.04 S cm^{-1}, compared to 0.5 S cm^{-1} for the standard electrolyte, as calculated from the correlation given by Hsueh and reported in [11]; hence, ohmic overpotential incidence on polarization measurements can be important for the high pH electrolyte. Therefore, only the overpotential increment upon additive addition at fixed cd, with respect to base electrolytes, is considered in the following.

The kinetic behaviour during deposition was investigated with the secondary current pulse (SCP) technique [12]. SCP measurements were performed in a standard three-electrode configuration, with a platinum RE, overimposing short (4 ms) square current pulses (30, 40, 50 and 70 mA cm^{-2}) during deposition at 20 mA cm^{-2}, 30 °C and without stirring. Before measurements, copper was deposited from the bath under study at 20 mA cm^{-2} for 30 min. Ohmic drop in solution, η_ω, could be readily determined from transients; a linear relationship between η_ω and ($i_P - i_D$) was found in all instances.

Table 1. Plating baths composition

Solution	A	A1	B	B1	E	G	H	L	N	C	F	Q
$CuSO_4 \cdot 5H_2O$/mol l^{-1}	0.8	0.8	0.8	0.8	0.8	0.8	0.8	0.8	0.8	0.25	0.25	0.25
H_2SO_4/mol l^{-1}	pH 3	0.5	pH 3	0.5	pH 3	pH 3	pH 3	pH 3	pH 3	1.5	1.5	1.5
Cl^-/ppm	–	–	50	50	50	50	50	50	50	50	50	50
1500MW PEG/ppm	–	–	–	–	–	300	300	–	300	–	300	300
TC/ppm	–	–	–	–	8	–	8	–	8	–	–	8
QAS/ppm	–	–	–	–	–	–	–	18	18	–	–	18

3. Results

3.1. *Linear sweep voltammetry*

Low scan linear sweep voltammograms for $CuSO_4$ 0.8 M solutions at pH 3 are shown in Figure 1. The addition of 50 ppm Cl^- shifts the curve 20–40 mV towards more negative potentials, depending on the current density; a lower polarization effect is observed during galvanostatic deposition (10 mV at 20 mA cm^{-2}). OCP measurements of copper in $CuSO_4$ 0.01 M solution at changing Cl^- concentration up to 100 ppm, show that, upon Cl^- addition, a negative shift of the equilibrium potential occurs at pH 3.5 or 2.8 (10 and 5 mV, respectively), while there is no effect upon OCP in H_2SO_4 0.4 M solution (in this case a corrosion potential is actually measured). This potential shift can be related to decreased activity of Cu^+ at the interface [13]. In low acid solutions, OCP changes appreciably only up to 30–40 ppm Cl^- concentration, whilst above about 100 ppm Cl^- ions trigger copper dissolution.

After addition of organic additives a polarization effect is always observed; Table 2 reports the overpotential increase in the presence of different additions, with respect to additives-free baths, during deposition at 20 mA cm^{-2}. Upon addition of PEG 300 ppm to bath B, the potential shifts about 0.2 V towards more negative values, in agreement with early findings [14, 15] and many recent reports. The addition of either TC 8 ppm (bath E) or QAS 18 ppm (bath L) gives a marked polarization effect as well; also the shape of the curves is affected, with a fast cd increase at similar potential. Steady state overpotential at 20 mA cm^{-2} is substantially higher for bath E than for bath L. Copper rest potential in bath E remains unchanged, while in the presence of QAS, potential decays almost linearly after current interruption and an equilibrium value is reached very slowly, showing a cathodic shift of about 50 mV with respect to bath B. Bath H, containing PEG 300 ppm and TC 8 ppm, conforms to bath G in the region of low to medium overpotentials; at higher overpotential, in the cd range of practical interest for plating, a remarkable

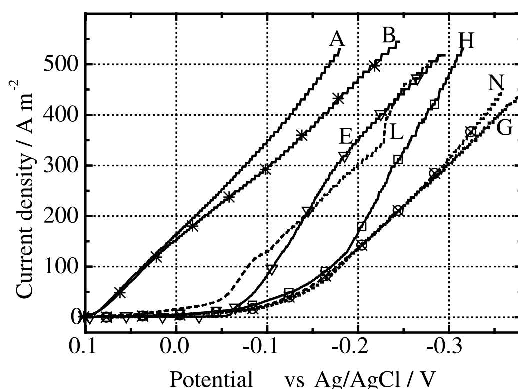

Fig. 1. Polarization curves (0.2 mV s^{-1}) at stationary copper electrode under magnetic stirring and 25 °C, from the various electrolytes given in Table 1.

depolarizing effect is observed, as shown by the slope increase of the i/E curve. In the presence of all additives (bath N), the shape of the curve corresponds strictly to the case of bath G, suggesting that, according to potentiodynamic measurements, the leading influence of PEG is restored by QAS addition. Linear sweep voltammograms performed on standard acidic baths in the presence of PEG and all additives present a similar behaviour with slightly higher polarization effects compared to pH 3 baths, whose magnitude is in good agreement with published data on different additives of the same chemical nature, as reported in [16].

3.2. *Transient electrokinetic behaviour*

The overvoltage transient at the growing surface during SCP measurements (Figure 2) is described by a two term equation: the first resulting from the equivalent circuit of the potentiometric cell, consisting of the parallel between a nonlinear resistor with Tafel characteristic and a variable adsorption capacitance; the second from a linearized Sand-type contribution. The following equation for the overpotential transient results:

$$\eta = B_T \ln\left[\left(\frac{i_P}{i_D}\right) - \left(\frac{i_P - i_D}{i_D}\right)\exp\left(-\frac{i_D t}{B_T C_{ads}}\right)\right] + \frac{RT}{zF} \times \sqrt{\frac{t}{\tau}} \tag{1}$$

where i_D and i_P are the deposition and pulse current densities, respectively. The parameters B_T (mV dec^{-1}) transient Tafel slope, C_{ads} (μF cm^{-2}) adsorption pseudo-capacitance, τ (ms) relaxation time, are determined by a nonlinear fitting procedure. B_T is related to the asymptotic value of the transient overpotential after charging; a steady value is not reached at the end of the pulse when concomitant phenomena appear to influence the cathodic faradaic process. In this case, B_T is determined from the time behaviour of the transient by taking into account also the second term of the overpotential in Equation 1. The capacitance behaviour at the electrodic surface is related to the nature and amount of electroactive species adsorbed at the electrode. We assume for the capacitive cd the expression $C_{ads}\exp(\eta/B_T) \times (d\eta/dt)$, in order to account for the influence of the surface overpotential η on the capacitance change at the electrode [17]. $\tau^{1/2}$ shows a linear relationship with the reciprocal of $(i_P - i_D)$, while the product $\tau^{1/2}$ times i_P is not constant; that is, the observed phenomena do not conform to the case of electrode process controlled by diffusion and must involve some faradaic relaxation effects [18].

Tables 3 and 4 list the electrokinetic SCP parameters for copper electrodeposition from $CuSO_4$ 0.8 M, pH 3 and $CuSO_4$ 0.25 M, H_2SO_4 1.5 M electrolytes, respectively. The ± limit reported in the Tables is the deviation from the average of 6 to 12 values, changing pulse cd.

Table 2. Overpotential increase after additives addition, with respect to additive-free bath A ($CuSO_4$ 0.8 M, pH 3) and C ($CuSO_4$ 0.25 M, H_2SO_4 1.5 M, Cl^- 50 ppm), depositing at 20 mA cm^{-2} and 25 °C from stirred solutions

Base composition	$CuSO_4$ · 0.8 M pH 3							H_2SO_4 1.5 M	$CuSO_4$ 0.25 M
Solution	B	E	G (no Cl^-)	G	L	H	N	F	Q
$\Delta\eta$/mV	10	90	160	180	120	150	190	230	250

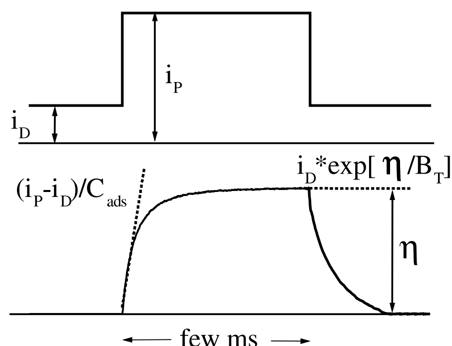

Fig. 2. Secondary current pulse (SCP) technique: a short current pulse, with cd i_P, is overimposed during galvanostatic deposition at cd i_D. Transient overpotential trace shown below, with graphical meaning of SCP parameters C_{ads} and B_T.

The transient behaviour of the pH 3 base electrolyte (bath A) is characterized by relatively low overpotentials, resulting in B_T values around 45 mV dec^{-1} and C_{ads} around 200 μF cm^{-2}. This is indicative of growth conditions with relatively easy discharge kinetics and high surface concentration of dischargeable species. Upon addition of Cl^- 50 ppm, the transient Tafel slope increases to 90 mV dec^{-1} and C_{ads} is reduced to about 90 μF cm^{-2} (values that can be compared with those found for the standard acid bath). A distinct feature of the transients profile in the pH 3 electrolytes is the overpotential increase after capacitive charging; the relaxation time τ is introduced to account for this effect, which becomes more important upon Cl^- addition. Values of the relaxation time τ are much lower compared to those for the standard acid electrolyte. Upon addition of H_2SO_4 0.5 M to pH 3 baths A and B, overpotential transients show a well defined plateau, that is, the relaxation effect disappears. In this case, Cl^- influence is almost nullified, pointing out the importance of electrolyte acidity on Cu^{2+} discharge.

Additives noticeably affect the transient behaviour. In the presence of TC (bath E), both B_T and C_{ads} increase with respect to bath B; the relaxation time τ is higher and steeply dependent on the pulse cd. The concurrent increase of the electrokinetic parameters points to a mere inhibiting effect of TC, in agreement with the results of the potentiodynamic analysis. QAS addition to bath B results in more appreciable changes of B_T (120 mV dec^{-1}) and C_{ads} (40 μF cm^{-2}), while τ values are close to those for bath B. Yet more significant changes are induced by PEG (bath G): B_T increases to 160 mV dec^{-1} and C_{ads} drops to 28 μF cm^{-2}, τ values remaining similar to those for bath B. In the case of the standard electrolyte, the effects of PEG addition (bath

Table 3. Electrokinetic SCP parameters for copper electrodeposition from $CuSO_4$ 0.8 M, pH 3 electrolytes at i_D 20 mA cm^{-2}, 30 °C, no stirring

Solution	Composition	B_T/mV dec^{-1}	C_{ads}/μF cm^{-2}	τ/ms
A	$CuSO_4$ 0.8 M pH 3	45 ± 15	195 ± 15	17 ÷ 0.3*
A1	$CuSO_4$ 0.8 M H_2SO_4 0.5 M	50 ± 5	85 ± 15	–
B	A + Cl^- 50 ppm	90 ± 15	90 ± 10	8 ÷ 0.2
B1	A1 + Cl^- 50 ppm	60 ± 10	80 ± 15	–
E	B + TC 8 ppm	100 ± 20	105 ± 5	78 ÷ 0.3
L	B + QAS 18 ppm	120 ± 10	40 ± 5	6 ÷ 0.35
G	B + PEG 300 ppm	160 ± 10	28 ± 2	7 ÷ 0.3
H	B + TC 8 ppm + PEG 300 ppm	140 ± 5	35 ± 5	9.7 ÷ 0.3
N	B + TC 8 ppm + PEG 300 ppm + QAS 18 ppm	90 ± 10	34 ± 5	19 ÷ 0.6

* The symbol ÷ indicates a decreasing range; thus, τ changes from 17 to 0.3 etc.

Table 4. Electrokinetic SCP parameters for copper electrodeposition from $CuSO_4$ 0.25 M, H_2SO_4 1.5 M electrolytes, at i_D 20 mA cm^{-2}, 30 °C, no stirring

Solution	Composition	B_T/mV dec^{-1}	C_{ads}/μF cm^{-2}	τ/ms
C	$CuSO_4$ 0.25 M H_2SO_4 1.5 M Cl^- 50 ppm	90 ± 10	110 ± 15	110 ÷ 11*
F	C + PEG 300 ppm	63 ± 5	30 ± 5	7 ÷ 1
Q	C + TC 8 ppm + PEG 8 ppm + QAS 18 ppm	65 ± 10	25 ± 5	10.5 ÷ 2.5

* The symbol ÷ indicates a decreasing range; thus, τ changes from 110 to 11 etc.

F) are quite different, with average parameters B_T 63 mV dec^{-1} and C_{ads} 30 μF cm^{-2}, which remain practically unchanged upon addition of the others additives. In the presence of both PEG and TC in the pH 3 bath, the change of B_T and C_{ads} shows that thiocompound addition to bath G promotes a slight kinetic activation, although PEG influence remains predominant. Such a mitigating effect on the suppressing action of the surfactant was already reported [19] and explained according to a model of 'local perforation' of the surfactant adsorbed barrier [8]. When all three additives are present, B_T is about 90 mV dec^{-1} and C_{ads} 34 μF cm^{-2}; τ values are close to those of the additives-chloride free electrolyte. The change of the transient Tafel parameter provides a clear evidence of the synergetic character of additives action: from 160 through 140 to 90 mV dec^{-1}, upon consecutive addition of PEG, TC, and QAS to bath B.

3.3. *Structure and morphology*

3.3.1. *Chloride and sulfuric acid influence*

Electrodeposition from bath A on Si/TiN/Cu [111] gives layers with faint [100] PO. Grain size is relatively large and shows poor uniformity; growth features are not well defined, apart from scattered square base pyramidal grains (Figure 3). Chloride addition to the pH 3 bath affects structure and morphology: epitaxial growth on the sputtered copper seed is favoured giving [111] textured layers, with volume fraction of [111] orientation (M_{111}) in the range of 0.70 to 0.75; grain size is slightly reduced and more uniform, with increased tendency to faceting and formation of triangular based pyramids, related to [111] texture, also with truncated apex, indicative of weak interfacial inhibition. The size of coherent scattering domains (CSD), from the half height width of (111) reflection according to Debye–Scherrer, increases from an average value of 85 to 95 nm in the presence of Cl^- 50 ppm. The CSD change is very small and its significance questionable, but it is suggestive of easier lateral growth, in agreement with chloride effects upon the surface structure of copper single crystal [20], related to the formation of ordered Cl^- overlayers on the (111) Cu surface [21, 22].

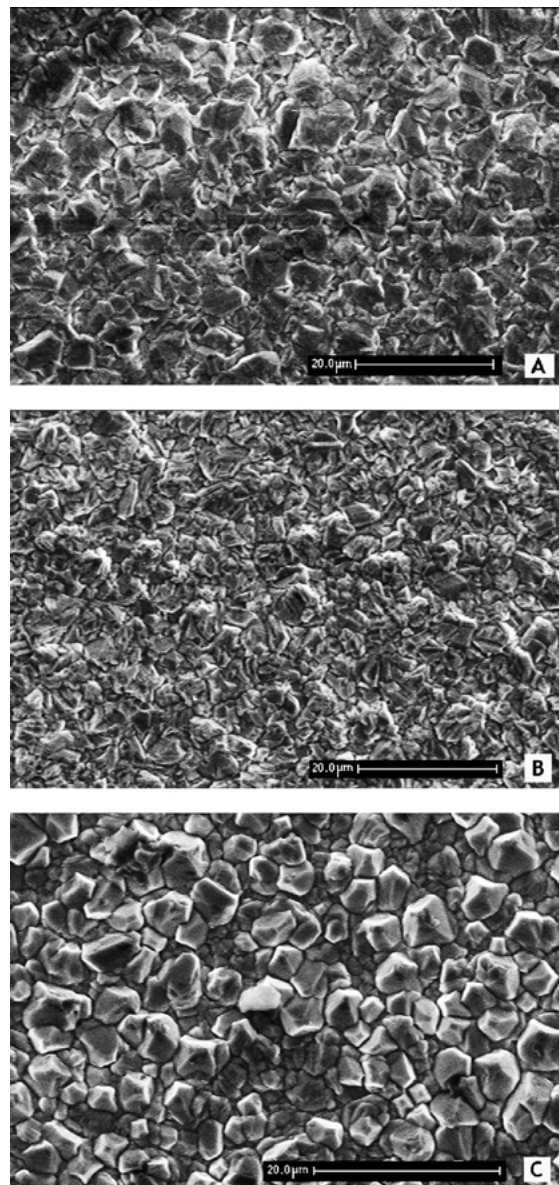

Fig. 3. Surface morphology of copper films from bath A, B and C (from top down); 30 °C, 20 mA cm^{-2}, stagnant electrolyte. Grains appear in the shape of square base pyramids on sample A and C ([100] textured) and of triangular base pyramids on sample B ([111] textured). Surface oxidation is visible on copper layers from pH 3 electrolytes.

Copper growth is also affected by H_2SO_4 0.5 M addition, in the absence of Cl^- (bath A1), depositing on brass substrate. CSD and grain size increase, with preferential growth of large pyramidal grains at sample edges, up to 20 μm in size for 10 μm thick deposits. Morphology is characterized by unshaped large grains related to a faint [100] PO. The addition of Cl^- 50 ppm (bath B1) mainly improves the [100] texture: the estimated volume fraction of grains in [100] direction is about 0.40 (no chloride) and 0.60 (50 ppm Cl^-). Macrothrowing power is definitely improved, while microroughness increases for 10 μm thick coatings, as previously reported [6]. Also in this case, Cl^- ions seem to sustain the base reproduction growth mode. On the contrary, high H_2SO_4 and low $CuSO_4$ concentration in bath C promotes the growth of weakly textured [100] layers on Si/TiN/Cu, with large rounded off pyramidal grains, in agreement with [23], showing that the increase of H_2SO_4 to $CuSO_4$ concentration ratio completely nullifies the Cl^- effect of preserving substrate orientation.

3.3.2. *Additive effect*

The [111] PO is weakened by all additives, compared to bath B, with the only exception of the thiocompound, which actually causes a slight improvement, increasing M_{111} up to 0.80. In Figure 4 M_{111} for copper layers deposited from additives containing solution (with the exclusion of bath E) is plotted against the overpotential increase at 20 mA cm^{-2} with respect to simple

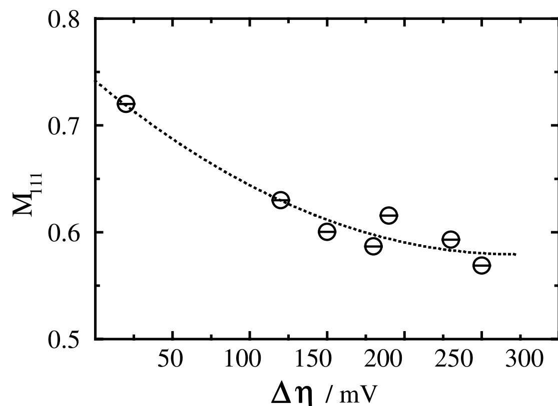

Fig. 4. M_{111}, [111] orientation volume fraction, of copper layers deposited from additives containing solution (with the exclusion of bath E) against the overpotential increase with respect to simple electrolyte (bath A).

electrolytes ($\Delta\eta$). No major difference results between low acid and standard acidic bath containing the three additives: [111] PO is only slightly higher for the pH 3 bath (bath N), compared to bath Q, with M_{111} about 0.61 and 0.57, respectively. The orientation dispersion effect can be related to the inhibition power of the additive package, confirming that the [111] PO is inherited from the substrate.

With regard to CSD size, TC addition induces no detectable decrease, compared to bath B, while in the presence of PEG alone and in combination with TC, CSD size is lowered down to 50–55 nm. Again, when all three additives are present (bath N), no appreciable change is observed. CSD size change versus $\Delta\eta$ (Figure 5) shows that [111] PO reduction is followed by CSD size decrease.

Figure 6 shows SEM micrographs of 10 μm thick copper deposits from baths with additives. When only PEG is present, a featureless surface structure develops, apart from growth features due to nodulation; in the presence of TC alone, the surface morphology shows uniform grains, 3 μm or less in size, with macro-twin

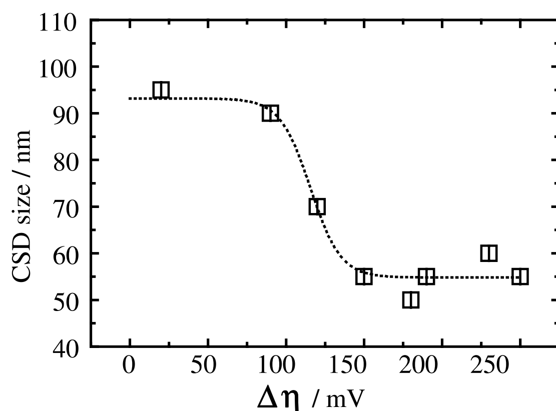

Fig. 5. Size of coherent scattering domains against differential overpotential due to single or combined additive addition (see data reported in Table 2).

planes. Surface morphology of copper films from bath H, in the presence of both PEG and TC, shows fine roundish crystals, of size down to 200 nm, with possible aggregation and a definite surface smoothening. The addition of QAS induces a slight grain size increase, up to 1 μm, with uniform growth features and an equiaxed fine grained structure, contrary to the typical columnar structure of deposits from additives free solutions (Figure 7).

3.4. *AFM imaging*

Full coverage of the substrate is not achieved after 30 s deposition at 20 mA cm^{-2} from the simple pH 3 bath, whilst, with Cl^- 50 ppm, substrate coverage occurs earlier and a compact and continuous layer is observed after 30 s deposition. AFM analysis reveals a surface spotted with relatively large, flat or pyramidal crystals, above a layer of roundish particles of less than 100 nm size (Figure 8), suggesting that crystal growth from bath B occurs with fast and diffuse nucleation, followed by preferential growth at active sites.

The addition of TC to bath B strongly modifies the growth characteristics and the crystal habit: faceted grains with twinning appear at the surface, resulting from the aggregation of very fine particles. PEG addition to bath B completely suppresses the preferential growth of isolated crystal, providing a self-evident picture of its strong inhibiting action; as a consequence, a surface structure smooth and uniform results. The combined effect of PEG and TC addition increases crystal size, whit growth features not well defined, mostly in the shape of round particles. QAS addition gives further changes, modifying grain morphology through formation of smooth, flat facets of relatively large extent, maintaining the same grain size as for bath G. These observations confirms the synergetic action of thiocompound and quaternary amine upon growth.

4. Discussion

The SCP technique was used to study the influence of electrolyte composition upon growth behaviour and the correlation between electrokinetics and structure. The surface conditions during growth are characterised in terms of macroscopic kinetic parameters, the transient Tafel slope B_T and the adsorption pseudo-capacitance C_{ads}, dependent on the degree of surface inhibition and electrocrystallization reactions. The possible occurrence of relaxation effects during the transients, related to either diffusive or adsorption phenomena, deserves further comments.

The transition time for Cu^{2+} diffusion is in the range from 20 to 2 s, for $CuSO_4$ 0.25 M solution, with cd from 20 to 70 mA cm^{-2}, with Cu^{2+} diffusion coefficient calculated according to the interpolation formula given by Quickenden and Jiang [24]. In the case of $CuSO_4$ 0.8 M solution at pH 3, even less important diffusive

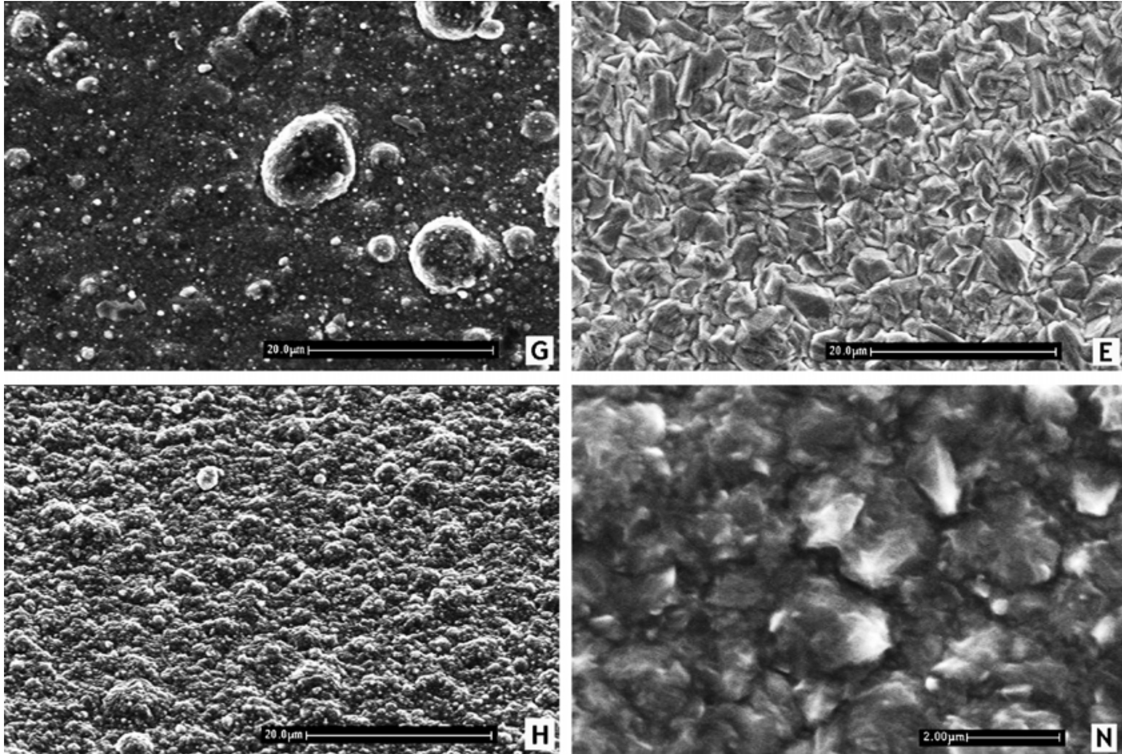

Fig. 6. Morphology of copper deposits from bath G, E, H and N (30 °C, 20 mA cm^{-2}, stagnant electrolyte). See Table 1 for bath composition.

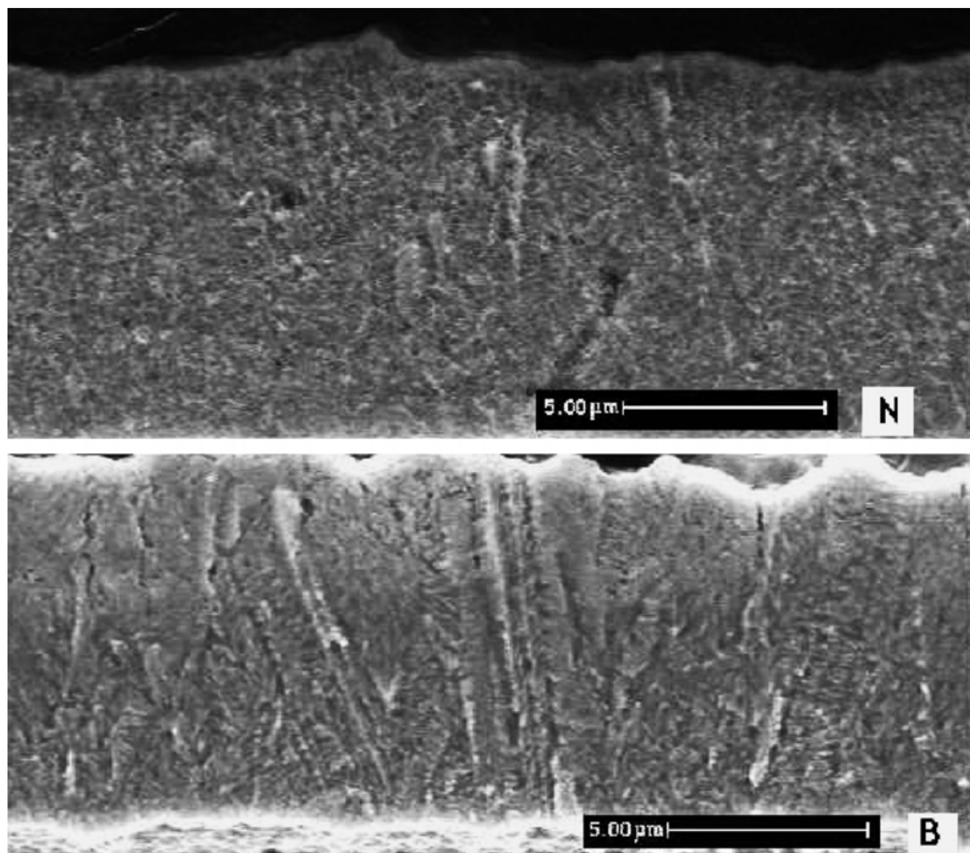

Fig. 7. Cross section of 10 μm thick copper deposits from bath B and N (stirred solutions, 25 °C, 20 mA cm^{-2}).

effects are expected because of lower concentration polarization and field induced enhancement of diffusion. With regard to Cu^+ reduction, its equilibrium concentration is very low and its actual concentration could be

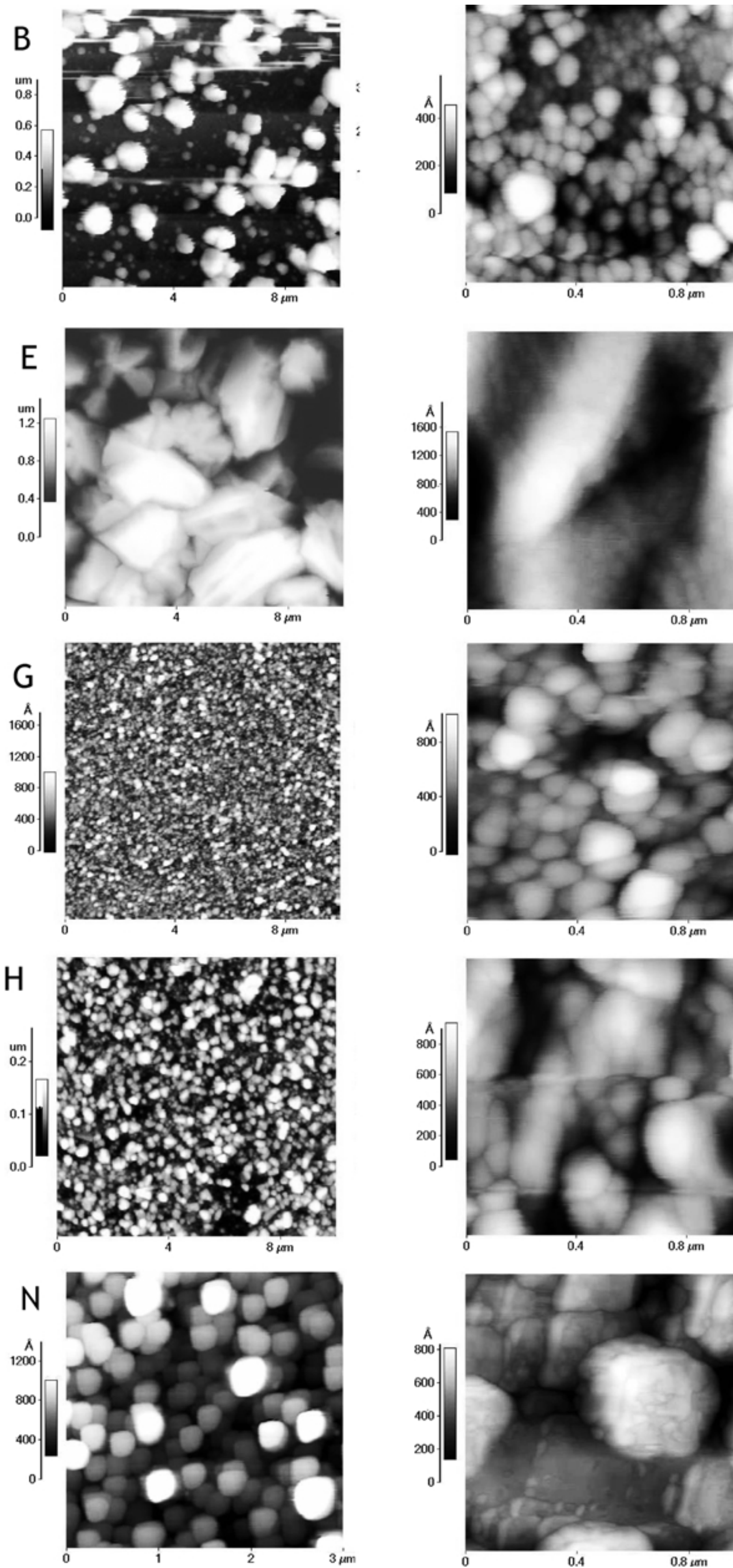

Fig. 8. AFM images of copper thin film after 30 s deposition at 20 mA cm^{-2} on Si/TiN/Cu 0.1 μm, 30 °C, no stirring. From top downward: bath B, E, G, H and N.

even lower: therefore, diffusion from the bulk solution is likely to give no or negligible contribution to its surface concentration. On the other hand, Cu^{+} is an intermediate in Cu^{2+} reduction and can accumulate at the

surface or diffuse back to the bulk solution. Therefore, diffusive transport cannot significantly affect the transient behaviour at the electrode. Thus, the second term in Equation 1 represents interfacial relaxation effects, related either to modification of the surface concentration of Cu^+ intermediates or to relaxation of additives surface coverage, depending on their adsorption and/or consumption. However, during the short transient time (4 ms), coverage by adsorbed additives is unlikely to undergo appreciable change, provided that additive consumption does not practically occur at the surface in such a short time; therefore, the observed behaviour can be attributed to surface relaxation of adsorbed Cu^+ intermediates. This interpretation is supported by results on the kinetics of the copper electrode [25], surface stability and accumulation of intermediates [26] and experimental accessibility of the charge transfer step Cu^+/Cu [27].

The growth behaviour during copper electrodeposition from pH 3, $CuSO_4$ 0.8 M electrolytes is determined by different and related factors: pH and copper concentration; additives, including chlorides, and their interaction. Their influence can be discussed with reference to the accepted mechanism of copper discharge [25]; that is, through their effects upon surface concentration and stability of Cu^+ intermediates generated by the rate-determining charge transfer step.

In standard baths the large sulfuric acid concentration has a great bearing upon discharge kinetics as well as growth structure and morphology. This influence is generally attributed to specific adsorption of sulfate anion [28], decreased Cu^{2+} ions activity, and increased concentration overpotential upon Cu^{2+} discharge [23]. In addition, the surface concentration of H^+ ions was shown to increase considerably with H_2SO_4 concentration [29], suggesting a specific influence of hydrogen surface coverage upon copper discharge kinetics. According to our results, high free acid content in the electrolyte has a twofold influence: a kinetic hindrance related to low Cu^{2+} concentration at the surface (relatively high B_T and C_{ads}) and a low stability of discharge intermediates, as inferred from τ values, that is, a fast ionic discharge step. Lowering acid content, down to pH 3, reduces surface inhibition, slightly favouring intermediates accumulation at the surface.

Chloride addition to the $CuSO_4$ 0.8 M pH 3 electrolyte affects the surface stability of intermediate species, in agreement with the impedance behaviour of copper in acidic sulfate solutions [30, 31]. Cu^+ ions activity is lowered, possibly through surface complexation, with inhibition of the ionic charge transfer step, slowing down of intermediates surface relaxation and activation of the surface towards nucleation and growth of new crystals; correspondingly, B_T and τ increase, C_{ads} decreases. Growth behaviour changes accordingly, with promotion of epitaxial or etero-epitaxial growth on [111] textured copper and [100] textured brass. The beneficial effect of Cl^- presence on epitaxial growth was already observed in the 'proper' case of deposition onto single crystals [30, 32].

The kinetic hindrance induced by Cl^- ions is also revealed by the overpotential increase during galvanostatic deposition or steady state polarization measurements, in agreement with the results of Chassaing and Wiart [30] for deposition from $CuSO_4$ 1.25 M, H_2SO_4 0.5 M solution. The opposite effect was reported for standard acid solutions [33] and for $CuSO_4$ 0.88 M, H_2SO_4 0.5 M solution, with a few ppm Cl^-, by Hill and Rogers [34]. More recently, the catalytic action of Cl^- traces upon the Cu^{2+}/Cu^+ reaction has been reported in 0.5 M $HClO_4$ solution [35]. This discrepancy on chloride kinetic effect can be explained taking into account a concomitant pH influence: the apparent Cl^- effect can actually be reversed from inhibition to activation, as electrolyte acidity increases.

The common feature of additive behaviour is their polarizing action, which leads to a distinct change in growth behaviour: higher overpotential enhances nucleation rate and depresses lateral growth rate, as reported for copper deposition in the presence of a quaternary ammonium salt and bromide on (111) gold single crystal [36], hence counteracting the preservation of the basis reproduction type growth. This is confirmed also by the relationship between M_{111} and CSD size against C_{ads}, shown in Figure 9: additive adsorption at the surface promotes nucleation and decreases growth activity, resulting in microstructure refinement and disruption of crystallographic coherence with the base. This is a point of concern, since texture can be a strict requirement for tailoring the properties of copper interconnects and its control becomes more important as features size keeps decreasing and occurrence of side-wall texture comes into question.

The effects of single additives or their combination are further discussed in the following. With regard to PEG influence, a possible interpretation must take into account the chemical interactions among PEG, metal ion and anions at the electrode. PEG produces a similar surface blocking effect if added to both starting electrolytes, through formation of an adsorbed barrier at the

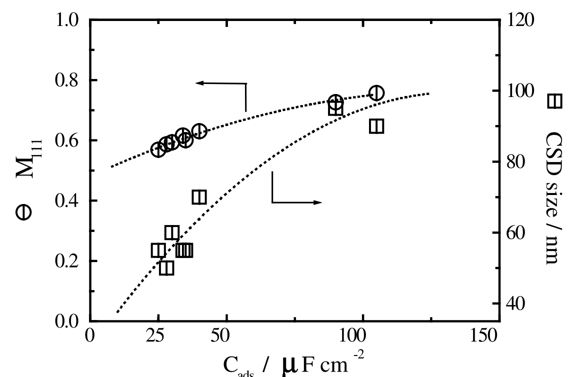

Fig. 9. Estimated [111] volume fraction and size of coherent scattering domains versus adsorption pseudo-capacitance values for $CuSO_4$ 0.8 M, pH 3 baths.

electrode and shrinkage of the available active area. In the case of the standard bath the adsorbed barrier at the electrode is merely a mechanical hindrance against copper ion transport [8, 15, 37] and surfactant adsorption appears to have a twofold effect: annihilation of the kinetic inhibition due to anions and hydrogen surface coverage, with lowering of B_T and C_{ads}, and increase of Cu^+ surface stability (i.e., inhibition of the ionic discharge step) as shown by the decrease of both C_{ads} and τ. Plating additives were reported to increase the Cu^+ level in acid sulfate bath [33] and a similar effect could be induced by PEG, as discussed in [14]. In the case of the pH 3 electrolyte, PEG addition displays peculiar effects, as revealed by the strong increase of B_T. Stable complex formation between PEG and Cu^+ ions was already envisaged by Hill and Rogers [14], similar to the case of cyclic polyether complexes with metal salts [38], giving molecular adducts between Cu^{2+} and PEG, which act as electron pair donor through its oxygen atoms. Complex formation could be favoured by both high copper concentration and pH, a possible consequence of slightly weaker cation–solvent and PEG–solvent interactions. However, based on OCP measurements at changing pH and PEG concentration, no evidence of Cu^{2+} complexation in bulk solution was found, in agreement with previous work [39], suggesting that complex species formation occurs at the surface in concomitance with Cu^+ stabilization. In these conditions, growth is under nucleation control through adsorption of dischargeable species, destabilising the base reproduction growth mode. Surface blocking leads to the development of a featureless morphology, with complete suppression of preferential growth of isolated crystals in the early stages of deposition, promoting structure refinement and surface levelling. Actually, the decrease of both [111] preferred orientation and CSD size appears a special consequence of PEG addition.

A key component of the additives system is the thiocompound and its effects are strictly related to the simultaneous presence of a blocking inhibitor such as PEG [8]. In fact, as shown by B_T and C_{ads} change upon TC addition to simple electrolyte, while being by itself a relatively strong kinetic inhibitor, the thiocompound behaves as an accelerator in the presence of PEG, due to its ability to displace selectively the suppresser and slightly reactivate the surface [19]. PEG–TC synergetic action could also be related to a lower surface stability of Cu^+ intermediates, as a result of a weak catalytic action of the thiocompound upon the ionic reduction step. Structural and morphological evidence for bath E may be qualitatively related to this behaviour: TC addition to the base solution containing 50 ppm Cl^- causes no appreciable decrease of CSD size; the volume fraction of [111] orientation is slightly increased or not affected, compared to deposits from base solution with chlorides, suggesting that the thiocompound stabilizes that same growth texture. In the presence of both PEG and TC, the best levelling and the most uniform thickness distribution are achieved, as already reported [6]. Besides, filling of 1:1 aspect ratio vias was successfully achieved only with a bath containing both additives, while the attempt to fill vias depositing from bath B or G was unsuccessful [6].

The quaternary ammonium salt influence, being a large molecule with low solubility and mobility, is the result of the interplay of diffusion and adsorption conditions. Strong selective blocking of the surface is observed, dependent on fluid flow and concentration, and, contrary to TC, no direct influence upon the ionic discharge step. On the other hand, the synergetic action between the quaternary ammonium salt and the other additives results in a slight surface reactivation, as shown by low values of both B_T and C_{ads}, possibly through a specific interaction with the thiocompound component. This is at variance with the result of the potentiodynamic analysis, suggesting that, this additive can actually modify or interfere with the kinetic mechanism of discharge.

5. Conclusions

Copper electrodeposition from pH 3 $CuSO_4$ 0.8 M electrolytes shows interesting, specific features in comparison with standard acidic baths.

Chloride plays a different role as additive in ‘no acid’ electrolytes, apart from its PEG subsidiary action [15], promoting epitaxial growth on [111] textured copper seed layer and structure refinement. These effects are weakened and eventually nullified by increasing the H_2SO_4 to $CuSO_4$ concentration ratio, as a possible result of surface inhibition by H^+ ion adsorption. In fact, high hydrogen surface coverage reduces the Cu^+ intermediate concentration at the interface, inhibiting nucleation and destabilizing the base-oriented reproduction growth. The tendency towards substrate texture maintenance is also weakened by organic additives, the only exception being the thiocompound.

Among additives, PEG plays the key role in determining both deposit microstructure and electrokinetic behaviour: as a consequence of the high inhibition level and supersaturation, growth occurs under nucleation control and possibly with cluster formation [40]. Lateral and epitaxial growth are no longer stable, because of prevailing adsorption interactions. Since a stronger surface interaction between PEG and reacting species is observed, with possible metal cation-PEG complex formation, the action of the surfactant becomes more effective in pH 3 electrolytes than in strongly acidic baths. The thiocompound effect on structure and morphology is related to its catalytic action on the ionic discharge step. The quaternary amine, although a strong inhibitor for copper electrodeposition, concurs synergistically with the thiocompound to the fine tuning of the ruling action of PEG. This could be a point of concern as long as the filling ability of the bath is concerned, while, on the other hand, it suggests the possibility of lowering the additive load in the bath, without detriment to its performance.

References

1. U. Landau, J. D'Urso, A. Lipin, Y. Dordi, A. Malik, M. Chen and P. Hey, *in* P.C. Andricacos, P.C. Searson, C. Reidsema-Simpson, P. Allongue, J.L. Stickney and G.M. Oleszek (Eds), 'Electrochemical Processing in ULSI Fabrication and Semiconductor/Metal Deposition II', PV 99–9, ECS Proceedings Series, Pennington, NJ (1999), pp. 25–40.
2. U. Landau, Ext. Abs. 53, 191st Meeting Electrochemical Society, Montreal, Canada, 4–9 May (1997).
3. K.M. Takahashi and M.E. Gross, *J. Electrochem. Soc.* **146** (1999) 4499.
4. S. Goldbach, B. van den Bossche, T. Daenen, J. Deconinck and F. Lapicque, *J. Appl. Electrochem.* **30** (2000) 1.
5. S.S. Kruglikov, *Russ. J. Electrochem.* **37** (2000) 776.
6. P.L. Cavallotti, R. Vallauri and A. Vicenzo, *in* AESF SUR/FIN 2000 Proceedings, AESF Inc., Orlando, FL (2000), pp. 325–333.
7. P.C. Andricacos, C. Uzoh, J.O. Dukovic, J. Horkans and H. Deligianni, *IBM J. Res. Develop.* **42** (1998) 567.
8. W. Plieth, *Electrochim. Acta* **37** (1992) 2115.
9. G.B. Harris, *Phil. Mag.* **43** (1952) 113.
10. M.H. Mueller, W.P. Chernock and P.A. Beck, *AIME Trans.* **212** (1958) 39.
11. R. Cabán and T.W. Chapman, *J. Electrochem. Soc.* **124** (1977) 1371.
12. P.L. Cavallotti, D. Colombo, U. Ducati and A. Piotti, *in* L. Romankiw, D.A. Turner, (Eds), 'Electrodeposition Technology, Theory and Practice' PV 87–17, ECS Proceedings Series, Pennington, NJ (1987), pp. 429–447.
13. U. Bertocci, *Electrochim. Acta* **11** (1966) 1261.
14. M. Hill and G.T. Rogers, *J. Electroanal. Chem.* **86** (1978) 179.
15. J.D. Reid and A.P. David, *Plat. Surf. Finish.* **74**(1) (1987) 66.
16. J.J. Kelly, C. Tian and A.C. West, *J. Electrochem. Soc.* **146** (1999) 2540.
17. K.E. Heusler, *Ber. Bunsenges. Phys. Chem.* **71** (1967) 620.
18. B.E. Conway, 'Theory and Principles of Electrode Processes' (Ronald Press, New York, 1965), p. 236.
19. R. Haak, C. Ogden and D. Tench, *Plat. Surf. Finish.* **69**(3) (1982) 62.
20. Q. Wu and D. Barkey, *J. Electrochem. Soc.* **147** (2000) 1038.
21. D.W. Suggs and A.J. Bard, *J. Am. Chem. Soc.* **116** (1994) 10725.
22. O.M. Magnussen and R.J. Behm, *MRS Bulletin* **24**(7) (1999) 16.
23. Y. Fukunaka, H. Doi, Y. Nakamura and J. Kondo, *in* L. Romankiw and T. Osaka (Eds), 'Electrochemical Technology in Electronics', PV 88-23, ECS Proceedings Series, Pennington, NJ (1988), pp. 83–93.
24. T.I. Quickenden and X. Jiang, *Electrochim. Acta* **29** (1984) 693.
25. E. Mattson and J.O'M. Bockris, *Trans. Faraday Soc.* **55** (1959) 1586.
26. R. Wiart, E. Lejay and F. Lenoir, *in* Proceedings of Interfinish, Basel, CH, Sept. 1972, Forster, Zürich, CH (1973), pp. 84–88.
27. T. Hurlen, G. Ottesen and A. Staurset, *Electrochim. Acta* **23** (1978) 39.
28. W. Dalla Barba and T. Hurlen, *J. Electroanal. Chem.* **91** (1978) 359.
29. K. Denpo, T. Okumara, Y. Fukunaka and Y. Kondo, *J. Electrochem. Soc.* **132** (1985) 1145.
30. E. Chassaing and R. Wiart, *Electrochim. Acta* **29** (1984) 649.
31. J.D. Reid and A.P. David, *J. Electrochem. Soc.* **134** (1987) 1389.
32. G. Carneval and J.B. De Cusminsky, *J. Electrochem. Soc.* **128** (1981) 1215.
33. L.S. Melnicki, *in* L. Romankiw and T. Osaka (Eds), 'Electrochemical Technology in Electronics', PV 88–23, ECS Proceedings Series, Pennington, NJ (1988), pp. 95–103.
34. M. Hill and G.T. Rogers, *J. Electroanal. Chem.* **68** (1976) 149.
35. Z. Nagy, J.B. Blaudeau, N.C. Hung, L.A. Curtiss and D.J. Zurawski, *J. Electrochem. Soc.* **142** (1995) L87.
36. E.D. Eliadis and R.C. Alkire, *J. Electrochem. Soc.* **145** (1998) 1218.
37. L. Mirkova, St. Rashkov and Chr. Nanev, *Surf. Technol.* **15** (1982) 181.
38. C.J. Pedersen, *J. Am. Chem. Soc.* **89** (1967) 7017.
39. S. Goldbach, W. Messing, T. Daenen and F. Lapicque, *Electrochim. Acta* **44** (1998) 323.
40. P.L. Cavallotti and A. Vicenzo, *in* D. Landolt, M. Matlosz and Y. Sato (Eds), 'Fundamentals of Electrochemical Deposition and Dissolution', PV 99–33, ECS Proceedings Series, Pennington, NJ (1999), pp. 123–134.